# Calibration of a finite element model of a borehole thermal energy storage in FEFLOW: model and numerical considerations

Karl W. Tordrup, Søren E. Poulsen and Henrik Bjørn

Centre of Applied Research and Development in Building, Energy & Environment,
VIA University College, 8700 Horsens, Denmark

kart@via.dk

**Keywords:** borehole thermal energy storage, numerical modelling, model calibration.

## ABSTRACT

We present operational data from a Borehole Thermal Energy Storage (BTES), and develop and calibrate a numerical temperature model of the thermal storage. Operational data from the initial 310 days form the basis for calibrating a 3D finite element model of the BTES. The model is subsequently validated by comparing temperature predictions for the following 200 days of operation to corresponding recorded measurements. We discuss modelling considerations and numerical issues encountered when attempting to calibrate and run a full finite element model for the BTES using the commercial software FEFLOW and present differences in predictions based on a simple thermal response test (TRT) versus the full finite element model.

## 1. INTRODUCTION

District heating currently supplies 62% of Danish consumers, and by 2035 heat production is to be based solely on renewable energy sources. To further advance the transition from fossil-based fuels to sustainable energy sources, large-scale thermal solar collector arrays are being integrated into the district heating networks in Denmark.

A 19,000 $m^3$ pilot Borehole Thermal Energy Storage (BTES) has been constructed by the district heating company in Brædstrup, Denmark in order to store excess heat production from an 18,600 $m^2$ thermal solar collector array. Heat is stored and abstracted from 48 Borehole Heat Exchangers (BHEs). The pilot project is aimed at evaluating the ability of the BTES for load balancing of the local district heating network. The BTES is scheduled to expand its storage volume to approximately 200,000 $m^3$, given that it performs in accordance with design targets.

The boreholes are arranged in a triangular grid and each borehole contains a 2U heat exchanger i.e. each borehole has two separate inlets and outlets (see Fig. 1). The 96 U-tubes are arranged in 16 strings, each with 6 U-tubes connected in series as indicated in Figure 2. The length of each borehole is 45 m and the

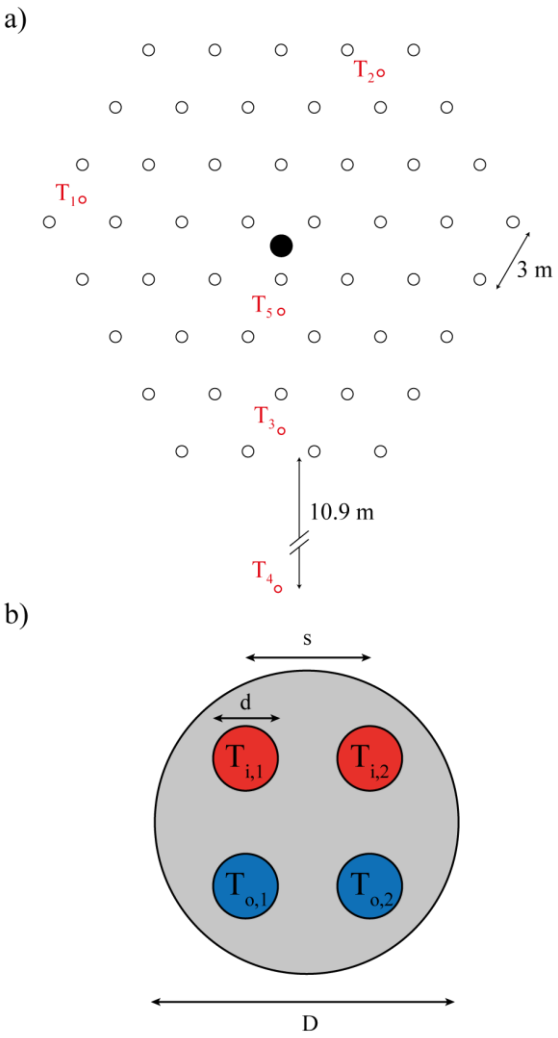


**Figure 1: a) BTES seen from above. Boreholes are indicated by black circles, temperature probes $T_1$ – $T_5$ by smaller red circles and the central manifold by a black disk. b) Cross section of a 2U heat exchanger showing the inlet and outlet of both U-tubes. The borehole diameter is D = 15 cm, the shank spacing is s = 6.2 cm, the U-tubes have outer diameter d = 3.2 cm and wall thickness 2.9 mm**

storage is overlain by 0.5 m mussel shells for insulation and finally 0.5 m soil fill. During charging, fluid flows from the centre of the storage and outwards, and during discharge the flow direction is reversed.

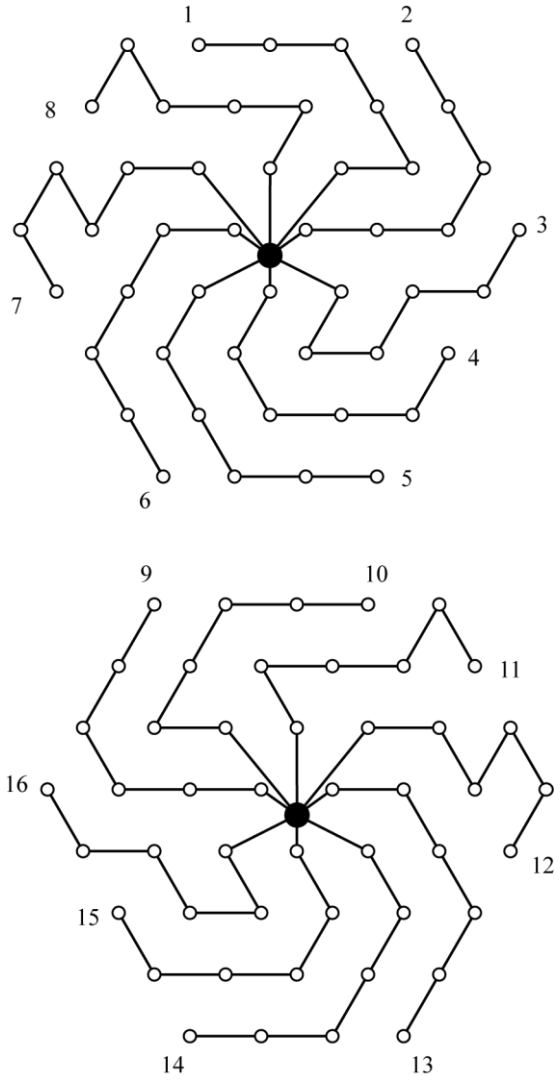


**Figure 2: Configuration of the first 8 BHE strings (top) and the last 8 strings (bottom). Note each borehole is part of two strings.**

Prior to operation the thermal conductivity of the soil was estimated from a standard thermal response test, yielding an estimated soil thermal conductivity of 1.42 W/m/K using the infinite line source interpretation (Gehlin and Hellström 2003). The volumetric heat capacity of the storage was estimated to 1.9 MJ/m$^3$/K using standard table values for soils similar to those found in the BTES.

## 2. OPERATIONAL DATA

Measurements of BTES temperatures and flow rates were recorded during the first 510 days of operation, together with inlet- and outlet temperatures for individual BHE strings. The flow is distributed evenly between all strings. In each of the temperature probe boreholes (see Fig. 1(a)) the soil temperature is recorded at 0, 1, 2, 3, 4, 9, 14, 19, 24, 29,34, 39, 44, 48, 49, 50, 51, 52, 53 and 59 m below the lower surface of the insulation. In Figure 3 we plot the measured inlet and outlet temperature and flowrate to the central manifold as well as representative temperature measurements in the subsurface inside and outside the BTES.

The temperature and flow measurements at the manifold display significantly higher frequency variation than the temperature response in the soil as would be expected. For the temperatures measured at $T_3$ (see Fig. 3(c)) we clearly see annual variation in temperature as the storage is charged during summer and discharged during winter, while the temperature response below the storage is moderate. Outside the storage at $T_4$ (see Fig. 3(d)) the temperature disturbance is moderate at the deeper levels, while the upper soil layers display larger annual variations due to insolation. Finally we note typical measurement logging errors which must be taken into account when attempting to model the storage. At $T_3$ a single measurement remains constant at 41.6 °C for 16 days during the second heating season and three out of the four time series exhibit a spike at $t$ = 498 d. Similar effects are observed at T4 where the measurement at 34 m below the insulation is constant at -20 °C for the first 244 days. For all measurements used in this study the amount of missing data points in each time series is less than 1%.

## 3. FINITE ELEMENT MODEL

We have developed a finite element model of the BTES using the commercial software FEFLOW. Based on the geological profile of the site, the model is divided into 6 layers as indicated in Figure 4. The upper boundary of the model corresponds to the lower boundary of the insulation i.e. the insulation is not included explicitly in the model.

The model domain extends vertically to 25 m below the BHEs and 20 m horizontally from the outermost BHEs. The horizontal extent of the model is chosen based on a simple line source model such that the temperature disturbance at the model boundary is negligible while the horizontal extent has been chosen based on trial and error. In all simulations performed in the present case temperature disturbances at the model boundary are less than 0.3 °C. The six nearest nodes to a BHE node are chosen at a distance of 6.13·D/2 = 0.46 m for optimum accuracy (Diersch et al. 2011). The remaining elements in the central storage region are of similar size, however outside the storage the node density is reduced by a factor of 4. This is to ensure that high temperature gradients in the storage volume are handled accurately without sacrificing computational time by over-discretizing the surrounding model volume where temperature gradients are smaller. In the vertical direction, a discretization of 1 m is used, corresponding to the minimum vertical distance between subsurface temperature measurements. Further increasing the vertical discretization was found to have negligible

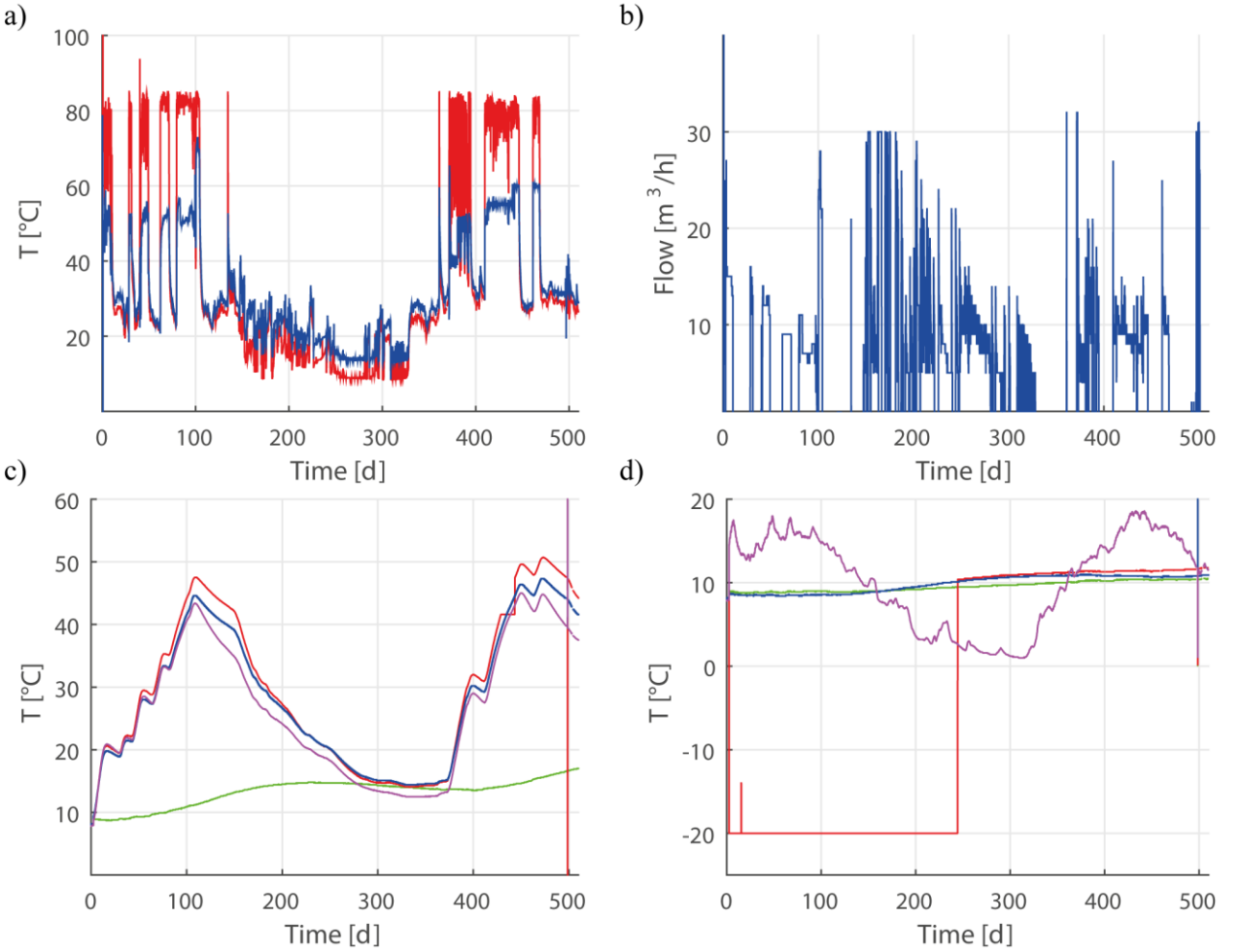


**Figure 3: a) Inlet (red) and outlet (blue) temperatures to the storage measured at the manifold. b) Total flowrate circulated in the storage. c) Temperatures at temperature probe $T_3$ measured at depths 1m (magenta), 14 m (blue), 34 m (red) and 50 m (green) below the insulation. d) Temperatures at temperature probe $T_4$ measured at the same depths as in c).**

influence on simulated temperatures. Automatic time step-step control is applied using the second-order accurate predictor-corrector scheme.

The model is driven by the measured BHE fluid flow rate and inlet temperatures. Since FEFLOW does not allow separate values for the inlet temperature of the two U-tubes in a 2U heat exchanger the model must be run separately for the two configurations in Figure 2. The final modelled temperature is the superposition of the temperatures calculated with the two models. Operational data are recorded at a resolution of 1 hour. These high resolution time series have an adverse effect on the runtime of the model, since it is forced to take relatively small time steps even though the temperature response in the soil occurs on a much longer time scale (see Fig. 3). Furthermore, it is unnecessarily demanding to remove outliers from the high frequency raw time series. Instead we aggregate all temperature measurements to daily averages. In order to ensure conservation of energy, the flow is subsequently aggregated as indicated in Eq. [1]

$$\dot{V}_l = \frac{1}{\sum_{i=1}^{16} \Delta T_{l,i} \Delta t} \int_t^{t+\Delta t} \sum_{i=1}^{16} \dot{V}_h \Delta T_{h,i} dt, \qquad [1]$$

where $\dot{V}$ is the volumetric flowrate, subscripts $h$ and $l$ refer to the raw high resolution data and low resolution aggregated values respectively, $\Delta T_{h,i}$ and $\Delta T_{l,i}$ are the difference between the inlet and outlet temperature for the $i$'th BHE array string in high and low resolution, respectively, and $\Delta t = 24\ h$ specifies the resolution of the aggregated data.

We have found that FEFLOW has difficulty handling the transition between zero and non-zero flow, with the temperature in the entire model volume increasing by twenty orders of magnitude in a single simulation step and the simulation essentially grinding to a halt. This can be remedied by inserting gaps in the time series to replace all zero-flow values. This approach essentially turns off the boundary condition at the BHE nodes.

When BHEs are connected in FEFLOW it is not possible to reverse the flow through the strings, i.e. we are not able to simulate the discharging of the BTES correctly since this proceeds from the outside of the storage volume. Instead we have developed a custom plug-in using the FEFLOW API (Application Programming Interface) to force the correct flow

direction under charging and discharging respectively, by explicitly linking the boreholes in the correct order in the two cases.

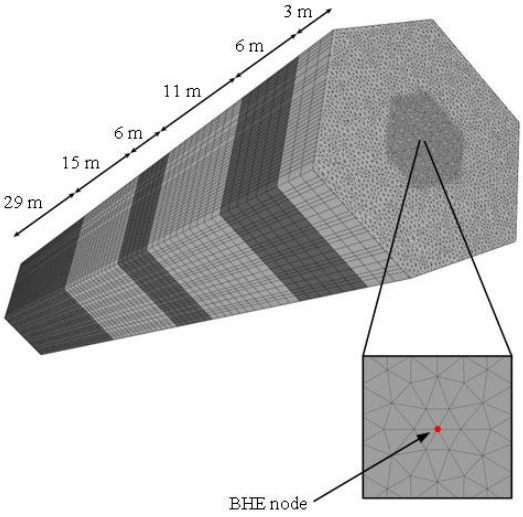


**Figure 4: Model mesh with geological layers indicated by alternating shades of grey.**

The BHEs are modelled using the quasi-stationary approach (Eskilson and Claesson 1988) to ensure reasonable simulation times. This implies the BHE flowrate should not vary significantly on a timescale set by the time needed to circulate fluid through the pipes and the line source time criterion $t = 5r_b^2/\alpha$, where $r_b$ is the borehole radius and $\alpha$ the thermal diffusivity.

We enforce a vanishing thermal gradient at the boundary of the model. This means that we assume the upper insulation is perfect and at the same time we neglect solar influx in the model. Since the dominant energy source in the storage volume is the direct injection and abstraction of heat through the BHEs this is not expected to affect the model significantly, however it does mean we cannot expect the model to be precise in the storage immediately under the insulation or outside the storage for the upper few meters where there is no insulation and the temperature is sensitive to insolation. Since all recorded temperatures in and around the storage volume prior to the first heat injection were between 7.9 – 8.2 °C the initial temperature is set to 8 °C in the entire model volume.

### 3.1 Model Calibration

The thermal conductivity and volumetric heat capacity of the six model layers shown in Figure 4 have been estimated using the optimization software PEST (Model-Independent Parameter Estimation) developed by Doherty (2016). Optimum model parameters are identified by minimizing the objective function

$$\varphi = \sum_{i=1}^{N_{probe}} \sum_{j=1}^{N_t} w_{i,j}(T_{i,j}^{(m)} - T_{i,j}^{(s)})^2 \qquad [2]$$

where $T^{(m)}$ and $T^{(s)}$ indicate measured and simulated temperatures respectively, $N_{probe}$ is the number of temperature probes, $N_t$ the number of temporal observations in the dataset for each temperature probe and $w_{i,j}$ is the weight assigned to individual observations. The initial guess for all layers is $\lambda$ = 1.42 W/m/K as suggested by the thermal response test and $\rho c$ = 1.9 MJ/m$^3$/K as estimated from table values. Operational data from the first 310 days of operation are used for minimizing Eq. [2]. For the first 20 days all weights ($w_{i,j}$ in Eq. [2]) are set to zero in order to allow initial transients to die out without affecting the optimization. For the remaining 290 days all weights are set to 1. The optimization is performed separately for the two configurations in Figure 2 and the final estimate is given as the average value for each layer. The optimized soil parameters are indicated in Table 1.

**Table 1: Estimated volumetric heat capacity and thermal conductivity for individual model layers.**

| Layer | $\rho c$ [MJ/m$^3$/K] | $\lambda$ [W/m/K] |
|---|---|---|
| 0 – 3 m | 2.03 | 2.27 |
| 3 m – 9 m | 2.27 | 1.39 |
| 9 m – 20 m | 1.75 | 1.63 |
| 20 m – 26 m | 2.15 | 1.48 |
| 26 m – 41 m | 1.94 | 1.75 |
| 41 m – 70 m | 1.86 | 2.44 |

The calibration is based on temperature measurements from 86 of the total 100 sensors at $T_1$ – $T_5$. The remaining 14 were rejected either because of measurement errors or because the sensors were too close to the boundary of the model where the effects of the insulation and insolation cannot be neglected.

### 3.2 Validation and Scaling

The calibrated model is validated by using the optimized parameters from Table 1 and comparing the temperature predictions to the corresponding observations for 200 days following the calibration period. The mean absolute deviation between measured and observed temperatures for all observation points inside the storage is $<|T^{(m)} - T^{(s)}|>$ = 1.46 °C and outside $<|T^{(m)} - T^{(s)}|>$ = 0.73 °C. These values cover significant variation within the model volume as indicated in Figure 5. Here we show the observed and simulated temperature at probe $T_2$ at 19 m below the insulation and probe $T_5$ at 2 m below the insulation where the mean absolute temperature deviation during the validation period is smallest respectively largest at 0.33 °C and 3.56 °C respectively.

With this variation in mind and considering the variation in estimated soil parameters from Table 1 it is pertinent to consider how well the model predicts the injected energy. For the full 510 days the observed accumulated energy injection is 616 MWh, the

calibrated model underestimates this figure by just 4 %. By contrast if we run the model assuming uniform geology with the initial estimates $\lambda$ = 1.42 W/m/K and $\rho c$ = 1.9 MJ/m$^3$/K, the accumulated energy is underestimated by 12.5 %. In other words we predict quite significant scaling effects when basing model projections on thermal response test estimates. The reason for this is that the thermal response test only samples a very small volume of the storage. In the present case, the test was run for 72 h, so from the initial estimates the characteristic thermal diffusion distance is just $l = \sqrt{\lambda t/\rho c} = 0.44$ m. Additionally the standard TRT interpretation does not allow stratification of the storage volume.

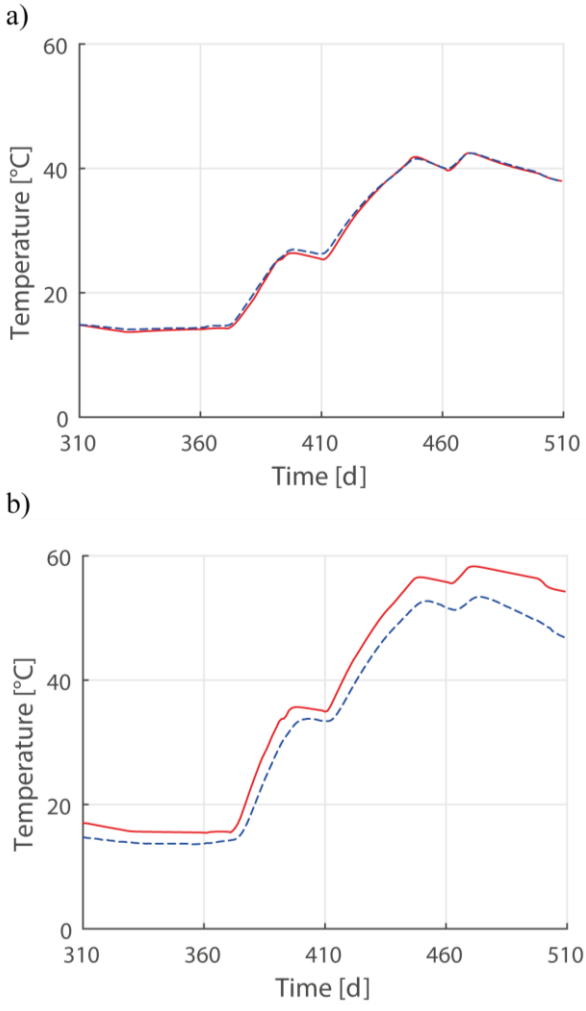


**Figure 5: a) Comparison of observed (solid) and simulated (dashed) temperatures for the observation point $T_2$ at 19 m below the insulation. b) Comparison of observed (solid) and simulated (dashed) temperatures for the observation point $T_5$ at 2 m below the insulation.**

Finally, we note that the calibrated model is to some extent sensitive to the pulse energy under both charging and discharging. The predictions improve with increasing pulse energy as can be seen in Figure 6. Since the simulation error tends to be larger for low energy pulses, these are disproportionally responsible for the final accumulated error.

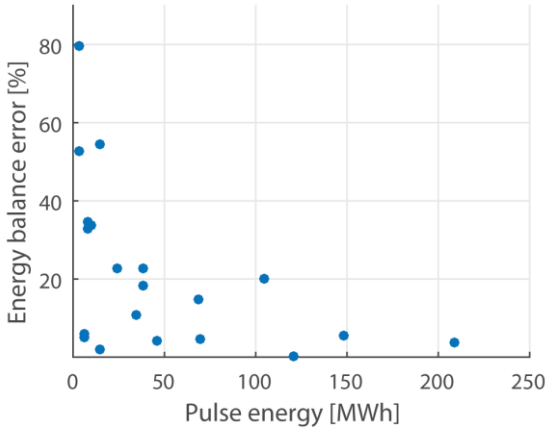


**Figure 6: The percentage difference between observed and simulated energy injection or abstraction for individual pulses (periods with non-zero flow) against pulse energy for the full 510 days dataset.**

We attribute this to a combination of numerical effects. Low energy pulses are generally shorter which increases the effect of how FEFLOW handles the transition between gaps and non-zero values in the measured flow through the boreholes. Additionally shorter pulses and pulses with low or varying flowrates are less suited for the quasi stationary model and hence incur relatively larger errors. While these numerical effects reflect areas where the model struggles to accurately represent the storage under the conditions it was actually operated, they do imply that for long term model projections it is advisable to inject and abstract energy in few high energy pulses in order to minimize the final prediction error.

## 4. CONCLUSION

In conclusion we have described, calibrated and validated a numerical FEM model of an operational pilot borehole thermal energy storage using the commercial software FEFLOW. In order to successfully calibrate the model it is important that the runtime not be too long. This implies there is a balance between how detailed the model should be e.g. grid coarseness and time series resolution on the one hand and computational time for optimizing the objective function on the other. Furthermore we have found that the calibration cannot be performed using FEFLOW as is, since features such as separate inlet temperatures for 2U heat exchangers and reversing the flow direction in BHE arrays are not provided.

Finally we have compared the full 3D FEM model predictions to those based on a standard thermal response test. We find that by including spatial and temporal information from recorded operational data from the pilot storage we effectively sample a much larger volume and thus are able to provide improved

predictions. Furthermore since simulation error is correlated with pulse duration it is preferable to base long term model projections on few pulses of long duration.

## REFERENCES

Diersch, H.-J.G., Bauer, D., Heidemann, W., Rühaak, W. and Schätzl, P.: Finite element modelling of borehole heat exchanger systems: Part 2. Numerical simulation, *Computers & Geosciences*, **37**, (2011), 1136-1147.

Doherty, J.: PEST. Model-Independent Parameter Estimation. User Manual Part I: 6th Edition, *Watermark Numerical computing*, (2016) http://www.pesthomepage.org/getfiles.php?file=newpestman1.pdf

Eskilson, P. and Claesson, J.: Simulation model for thermally interacting heat extraction boreholes, *Numerical Heat Transfer*, **13**, (1988), 149-165.

Gehlin, S. E. A. and Hellström, G.: Comparison of Four Models for Thermal Response Test Evaluation, *ASHRAE Transactions*, **109**, (2003), 131-142.